

The Automatic Alignment System for the Virgo Interferometer

F. Acernese⁶, P. Amico¹⁰, M. Al-Shourbagy¹¹, S. Aoudia⁷, S. Avino⁶, D. Babusci⁴,
G. Ballardini², F. Barone⁶, L. Barsotti¹¹, M. Barsuglia⁸, F. Beauville¹, M.A. Bizouard⁸,
C. Boccardi⁹, F. Bondur⁷, L. Bosi¹⁰, C. Bradaschia¹¹, S. Braccini¹¹, A. Brillet⁷, V. Brisson⁸,
L. Brocco¹², D. Buskulic¹, E. Calloni⁶, E. Campagna³, F. Cavalier⁸, R. Cavalieri², G. Cella¹¹,
E. Chassande-Mottin⁷, C. Corda¹¹, A.-C. Clapson⁸, F. Cleva⁷, J.-P. Coulon⁷, E. Cuoco²,
V. Dattilo², M. Davier⁸, R. De Rosa⁶, L. Di Fiore⁶, A. Di Virgilio¹¹, B. Dujardin⁷, A. Eleuteri⁶,
D. Enard², I. Ferrante¹¹, F. Fidecaro¹¹, I. Fiori¹¹, R. Flaminio^{1,2}, J.-D. Fournier⁷, S. Frasca¹²,
F. Frasconi^{2,11}, A. Freise², L. Gammaitoni¹⁰, A. Gennai¹¹, A. Giazotto¹¹, G. Giordano⁴,
L. Giordano⁶, R. Gouaty¹, D. Grosjean¹, G. Guidi³, S. Hebri², H. Heitmann⁷, P. Hello⁸,
L. Holloway², S. Kreckelbergh⁸, S. Karkar¹, P. La Penna², N. Letendre¹, V. Lorette⁹,
M. Loupas², G. Losurdo³, J.-M. Mackowski⁵, E. Majorana¹², C. N. Man⁷, M. Mantovani¹¹,
F. Marchesoni¹⁰, F. Marion¹, J. Marque², F. Martelli³, A. Masserot¹, M. Mazzoni³, L. Milano⁶,
C. Moins², J. Moreau⁹, N. Morgado⁵, B. Mours¹, A. Pai¹², C. Palomba¹², F. Paoletti^{2,11},
S. Pardi⁶, A. Pasqualetti², R. Passaquieti¹¹, D. Passuello¹¹, B. Perniola³, F. Piergiovanni³,
L. Pinard⁵, R. Poggiani¹¹, M. Punturo¹⁰, P. Puppo¹², K. Qipiani⁶, P. Rapagnani¹², V. Reita⁹,
A. Remillieux⁵, F. Ricci¹², I. Ricciardi⁶, P. Ruggi², G. Russo⁶, S. Solimeno⁶, A. Spallicci⁷,
R. Stanga³, R. Taddei², M. Tonelli¹¹, A. Toncelli¹¹, E. Tournefier¹, F. Travasso¹⁰, G. Vajente¹¹,
D. Verkindt¹, F. Vetrano³, A. Viceré³, J.-Y. Vinet⁷, H. Vocca¹⁰, M. Yvert¹ and Z.Zhang²

¹ Laboratoire d'Annecy-le-Vieux de physique des particules Chemin de Bellevue - BP 110, 74941
Annecy-le-Vieux Cedex - France ;

² European Gravitational Observatory (EGO), Via E. Amaldi, I-56021 Cascina (PI) Italia;

³ INFN - Sezione Firenze/Urbino Via G.Sansone 1, I-50019 Sesto Fiorentino; and/or Università di Firenze,
Largo E.Fermi 2, I - 50125 Firenze and/or Università di Urbino, Via S.Chiera, 27 I-61029 Urbino, Italia;

⁴ INFN, Laboratori Nazionali di Frascati Via E. Fermi, 40, I-00044 Frascati (Roma) - Italia;

⁵ LMA 22, Boulevard Niels Bohr 69622 - Villeurbanne- Lyon Cedex France;

⁶ INFN - Sezione di Napoli and/or Università di Napoli "Federico II" Complesso Universitario di Monte
S. Angelo Via Cintia, I-80126 Napoli, Italia and/or Università di Salerno Via Ponte Don Melillo, I-84084
Fisciano (Salerno), Italia;

⁷ Department Artemis - Observatoire de la Côte d'Azur, BP 42209, 06304 Nice Cedex 4, France;

⁸ Laboratoire de l'Accélérateur Linéaire (LAL), IN2P3/CNRS-Université de Paris-Sud, B.P. 34, 91898
Orsay Cedex - France;

⁹ ESPCI - 10, rue Vauquelin, 75005 Paris - France;

¹⁰ INFN Sezione di Perugia and/or Università di Perugia, Via A. Pascoli, I-06123 Perugia - Italia;

¹¹ INFN - Sezione di Pisa and/or Università di Pisa, Via Filippo Buonarroti, 2 I-56127 PISA - Italia;

¹² INFN, Sezione di Roma and/or Università "La Sapienza", P.le A. Moro 2, I-00185, Roma.

E-mail address: maddalena.mantovani@ego-gw.it

Abstract

The French-Italian interferometric gravitational wave detector Virgo is currently being commissioned. Virgo is a Michelson interferometer with 3 km long arm cavities and a power-recycling mirror.

The optical elements are suspended by so-called *super-attenuators*, which provide an excellent isolation in the range above the resonances frequencies of the mechanical system. To achieve the high sensitivity needed for such a kind of experiment the positions of all the suspended mirrors have to be continuously controlled, using optical signals derived from the main beams of the interferometer.

In this paper we give a description of the automatic angular control system currently used in Virgo, with emphasis on the optical design and the control topology. We report on

the first experimental implementation of the Anderson-Giordano technique in a large scale interferometer and its performance during recent data taking periods.

1 Introduction

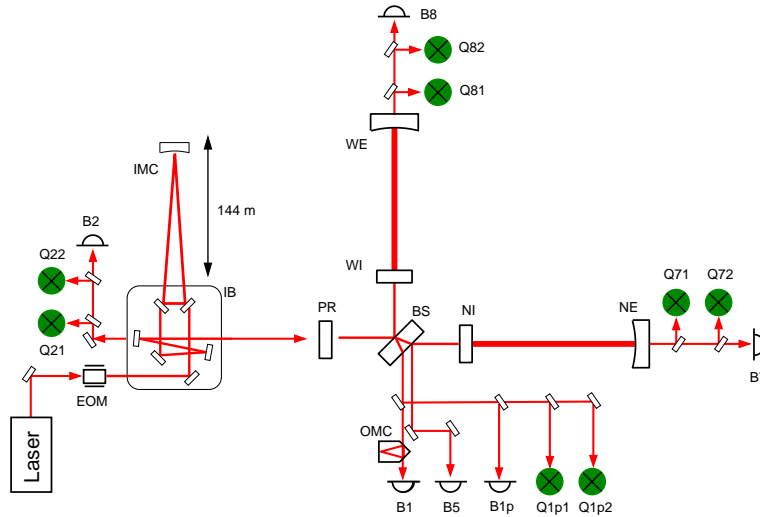


Figure 1: A simplified scheme of the optical design of Virgo in the final configuration. The photodiodes used for longitudinal (labeled with **B**) and alignment (labeled with **Q**) control systems are shown. The output port signal is taken from B1.

One of the most interesting predictions of Einstein's theory of general relativity is the existence of gravitational waves (GW). Several large GW detectors have been developed around the world, aiming at the first direct detection of gravitational waves with a long term goal of observing and probing the physics of massive objects in the universe.

The Virgo interferometer is a ground-based interferometric gravitational wave detector constituted mainly by a Michelson interferometer (ITF). Resonant optical techniques (like 3 km long Fabry-Perot cavities in the interferometer arms) are used to enhance the sensitivity to gravitational waves.

The main optical components are isolated from the ground motion by a system of controlled mechanical suspensions, which strongly reduce all displacement noises of the mirrors in a frequency range well above the suspensions main resonances (> 10 Hz). Thus the mirror behave as *free-falling test masses* suitable for detecting the metric perturbation due to gravitational waves. Given the optical layout shown in Fig. 1, gravitational waves propagating orthogonally to the interferometer plane would produce a signal, due to interference pattern change, at the output port.

The design sensitivity of the Virgo is limited by the noise sources affecting the system and it is remarkable even at low frequency, being the detection bandwidth 10 Hz-few kHz [1]. In terms of linear spectral density of metric perturbation strain the sensitivity is $h < 10^{-22}/\sqrt{Hz}$ at 100 Hz, which corresponds to a residual rms displacement of the mirrors $\Delta L < 3 \cdot 10^{-19}$ m over 1 Hz bandwidth.

2 Optical layout of the Virgo interferometer

The optical scheme of Virgo is shown in Fig. 1. A laser beam generated by a Nd:YAG solid state laser with 22 Watt of power and wavelength of $\lambda = 1064$ nm is split at a *beam splitter* mirror (BS) in two beams which are injected to the two orthogonal arm cavities (North arm and West arm). The beams reflected by these cavities are then recombined at the BS. The longitudinal position of all the mirrors are controlled in such a way that this recombination creates a destructive interference

Mirrors	RMS [rad]
Power Recycling Mirror	10^{-7}
Input Mirrors	$2 \cdot 10^{-8}$
End Mirrors	$3 \cdot 10^{-9}$

Table 1: Requirements of total RMS motion for all the mirrors.

in the main output port, called *dark fringe*. In this condition almost all the light power is reflected back to the *power recycling mirror* (PR). The presence of this mirror allows to enhance the power circulating in the interferometer. The light from the dark port of the beam splitter is filtered by an *output mode cleaner* (OMC) before being detected by a set of high-sensitivity photo diodes. The dark fringe signal, detected read-out before the OMC is strongly affected by the alignment of the Fabry-Perot cavities and then it is very practical to use it in an alignment servo-loop.

In order to be able to consider the test masses as free, all of the main optics are suspended in an ultra-high vacuum by a complex system called *super-attenuator* (SA) [1], which strongly reduces the seismic noise injected to the mirrors. The super-attenuator is constituted by a long pendulum and several seismic filters. The last filter stage, from which the mirror and a so-called *reference mass* are suspended, is called *marionette* [2]). The SA system provides a seismic noise suppression of $\approx 10^{-12}$ at a few Hz. Longitudinal and angular forces can be applied to the mirror and to the marionette by using coil-magnet actuators.

In order to be able to detect a GW signal the fluctuation of the mirror relative positions should be of the order of picometers; for this reason a longitudinal and angular mirror control has been developed.

The control systems are based on a modulation-demodulation technique: the input beam is modulated in phase before it enters the *input mode cleaner* (IMC) using an *electro-optic modulator* (EOM), at a modulation frequency of about $f_{RF} = 6.26$ MHz. This modulation can be described as creating new components in the light field, which are frequency shifted by offsets $\pm f_{RF}$ with respect to the *carrier* at f_0 (the new components are usually called *upper* and *lower sideband* respectively). Demodulating the signals coming from photo-detectors placed on the main beams at f_{RF} yields position information for the interferometer components. The longitudinal control system is usually referred to as the *locking system* [3].

3 Automatic Alignment control strategy

A misalignment of the mirror with respect to the beam produces a variation on the effective arm length of the interferometer which can mimic the effect of a GW passage. Thus, to obtain the high sensitivity required by a detector like Virgo, the residual mirror angular motion of the mirrors must be reduced down to some n rad (see Table 1). The *automatic alignment* (AA) is a servo-loop system designed to reduce the fluctuations of the mirror angular motions with respect to the beam, thus maintaining the overall alignment of the optical elements and reducing the noise at the dark fringe port.

In order properly control all the angular degrees of freedom, a scheme for getting angular error signals has been designed carefully, taking into account the parameters of the interferometer. The optical design of the Virgo interferometer is based on the *Anderson-Giordano technique* [4, 5], a variant of the Anderson technique [6]. We are using four beams coming out of the interferometer to construct useful angular error signals. They are: the main beam reflected by the ITF, the two beams transmitted at the end of the long arm cavities, and the pick-up beam at the secondary surface of the BS (see Fig. 1). The main feature of the Anderson-Giordano technique is the fact that all the detection ports are able to detect the motions of all mirrors. In addition, the Virgo control system uses only one modulation frequency to generate the error signals for controlling both longitudinal and angular degrees of freedom.

The sensors for the alignment control are *quadrant split photo detectors* (or *quadrant photo-diodes* for short). These are photo-diodes with 4 separate elements. Each quadrant diode can

provide four signals: the sum over four quadrants gives the same signal as a normal photo-diode. The differences between the upper and lower elements and the left and right elements are computed and give the vertical and horizontal positions of the beam on the diode and serve as error signals for the diode centering. Demodulation of the differential quadrant diode outputs at f_{RF} yields two additional signals (in-phase and quadrature) that contain information about the angle and position (vertical and horizontal respectively) of the phase front of the carrier with respect to the sidebands.

Four sets of two quadrant diodes each are located on the most important beams coming from the ITF, as it shown in Fig. 1. Moreover the quadrant diodes are set, by a system of telescopes, to difference phases which gives us different signals; for each detection port we obtain therefore 4 signals.

Preliminarily all the mirrors are aligned by means of auxiliary devices, (*Local control* (LC) [7]) designed to drive mirror alignment, without exciting the suspension mechanics, until the interferometer is dark-fringe locked. Then, if the fluctuations of the alignment are reduced to fractions of μrad the automatic alignment can be enabled. The local control system has an accuracy of about $0.3 \mu\text{rad}$ within 5 Hz bandwidth, but when the mirrors are under Local Control the alignment drifts away even largely (up to about $1\text{-}2\mu\text{rad}/\text{hour}$), preventing a stable operation of the interferometer.

The goal of the automatic alignment system developed for the Virgo interferometer is to control the angular pitch and yaw motion of the six main mirrors (PR, BS, NI, NE, WI, WE), using, as shown in Fig. 1, four detection ports i.e. 16 demodulated error signals for each angular direction.

The relation between the set of quadrant photo-diode signals and the set of mirror tilts is expressed by a 16×6 optical matrix [8], whose elements can be directly measured by injecting calibrated sinusoidal excitations through the marionette actuators [1]. A χ^2 based inversion of the optical matrix [5] then yields a control matrix that is applied by the *Global Control* to the set of quadrant photo-diode signals to reconstruct the misalignment of each mirror. These misalignment signals are sent as error signals to *Digital Signal Processors* (DSP), which apply filters to build correction signals for the marionette actuators. The control bandwidth of the AA servo-loops is about 3 Hz.

4 Experimental results

During the commissioning of Virgo, the first AA configuration tested was developed to operate without power recycling (see Fig. 1: the PR mirror largely misaligned so that its reflected beam does not interfere into the interferometer). This is a relatively simple setup because the misalignments of the two arm cavities are decoupled, therefore the optical matrix is reduced to two 4×2 matrices, one for each cavity arm, for pitch and yaw motion. The commissioning of the automatic alignment system in this configuration was completed on May 2004 [9].

Before the implementation of the AA system for the full configuration we developed a slow *drift control system* in order to increase the duration of stable operation of the interferometer, which was mainly limited by slow drifts of the mirror positions. These drifts could not be corrected by a control system based on local ground references. Using the optical signals from the quadrants we implemented control loops with a very narrow bandwidth (a few mHz) to readjust the setpoint of the local control system, which remain enabled all times. In this way the local control reduces the high frequency angular fluctuations, while the slow motions are controlled through the global control system. This implementation is rather simple because its narrow bandwidth makes it less sensitive to signal couplings and not strongly affected by loop instability issues.

Our studies showed that it is better to describe the angular misalignment of the interferometer not using the motion of single mirrors, but, instead linear combinations of them which are the physical *normal modes* of the interferometer misalignments (see Table 2). Not all these modes have the same relevance for the stability of the interferometer; for example, the first mode of Table 2 (*differential mode of end mirrors*) is the most important one for the power stability of the

θ_x		θ_y	
NE - WE		NE + WE	
- PR + NI + WI + NE + WE		- PR + NI - WI + NE + WE	
NI - WI		NI + WI	
-PR - NI - WI + NE + WE		-PR - NI + WI + NE - WE	
PR + NI + WI + NE + WE		PR + NI - WI + NE - WE	

Table 2: Normal modes of the interferometer misalignment. The direction of rotation is referred to the front side of the optical component defined by the high-reflective coating

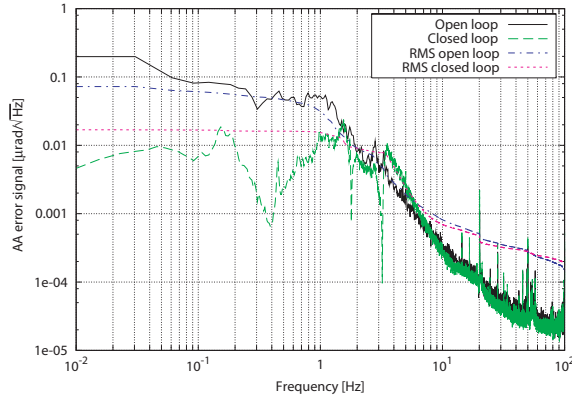


Figure 2: Comparison between the automatic alignment error signal for the North input mirror (θ_x) when the mirror is controlled by local control and by automatic alignment (*full configuration*).

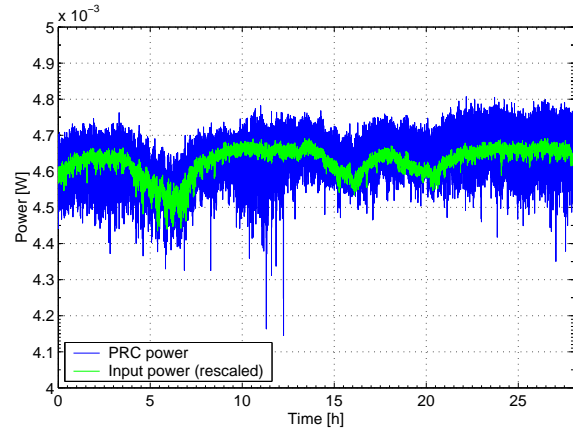


Figure 3: Trend of the power stored in the recycling cavity during 30 hours of lock with 10 AA control loops active, compared with the power transmitted by the input mode cleaner.

dark fringe port. Then, in this intermediate configuration we servoed the tilt of the NE mirror (see Fig. 1) directly by means of the dark fringe signal leaving the BS under local control and all the other mirrors under local control plus drift correction.

The full drift control system has been successfully implemented and tested during the last commissioning run (C6, from 29th of July to 12th of August). The entire interferometer was kept continuously well aligned and locked on the dark fringe, for slightly more than 40 hours, and after each unlock (due to reasons not related to alignment) there was no need to repeat the pre-alignment procedure. During these long periods the power stored in the cavity remained very stable; the residual long term fluctuations were mainly due to input beam jitter. The corrections on the mirror positions during this time were typically of the order of a few μrad .

The automatic alignment control system for the final configuration is still in the commissioning phase. Since August 2005 we managed to close 10 out of 12 automatic alignment control loops in a stable way leaving only one mirror (WI or BS) under LC. The remaining degrees of freedom refer only to the long-term stabilization of the beam position drift in the two arms. Thus the full high-gain (or high-frequency) section of the control system has been successfully integrated. A dedicated engineering data run has been scheduled to test and document of the interferometer in this condition.

The Fig. 2 shows the comparison between the NI mirror error signal spectrum of the local control system (dark-solid curve) and of the automatic alignment system (light-dashed curve); this comparison permits to us to have a cross calibration of the two signals. The noise reduction for the AA error signal below the unity gain frequency (u.g.f.) with respect with the LC error signal is due to a smaller electronic noise. Below the u.g.f the mirror motions is suppressed by the AA system. Integrating this spectrum it turned out that we are just below the requirements for what concerns the total RMS motion.

The Fig. 3 shows a trend of 30 h of continuous lock while 10 AA control loops were closed; the

dark curve represents the power stored in the recycling cavity and the light curve represents the rescaled input power; the comparison between the two shows that the power fluctuations in the interferometer are mainly due to the input power fluctuations.

This result is still preliminary, since for a complete study of performance and noise contribution it is necessary to have all the loops closed (12 d.o.f.). With this partial configuration the error signal for the control of each mirror has a big noise contribution from the angular motion of the WI mirror (which is not globally controlled). We expect that once all the mirrors are controlled by the automatic alignment system the main noise contribution to the error signals will come from the angular fluctuation of the injected beam (jitter). Moreover the plan is also to control slow drifts of the input bench and to implement in a future time a slow drift control, using the position of the beam on the quadrants located at the end of the North arm.

5 Conclusions

The implementation of an automatic alignment system, based on the Anderson-Giordano technique, on a large-scale interferometer has been successfully demonstrated. For the interferometer configuration with no power recycling an AA system was developed for the arm cavities and proved to be very robust. It is now used routinely as a part of the ITF pre-alignment procedure.

We implemented a drift control system which allowed more than 39 hours of continuous stable lock during the C6 commissioning run. This system provides a strong reduction of the power fluctuations in the dark fringe and a very good long term stability. For the full configuration, i.e. that with the PR mirror aligned, the automatic alignment is still under commissioning; we managed to close 10 out of 12 loops with good preliminary performance.

References

- [1] F. Acernese *et al.* [Virgo Collaboration], “Status of Virgo”, submitted to *Journal of Physics: Conference Series (Amaldi 6)*.
- [2] F. Acernese *et al.* [Virgo Collaboration], “The last stage suspension of the mirrors for the gravitational wave antenna Virgo”, *Clas. Quant. Grav.* **21**, 425-432 (2003).
- [3] F. Acernese *et al.* [Virgo Collaboration], “The Variable Finesse Locking technique”, submitted to *Journal of Physics: Conference Series (Amaldi 6)*.
- [4] D. Babusci, H. Fang, G. Giordano, G. Matone, L. Matone, V. Sannibale, “Alignment procedure for the Virgo interferometer: experimental results from the Frascati prototype”, *Phys. Lett. A* **226**, 31–40 (1997).
- [5] F. Acernese, *et al.* [Virgo Collaboration] “The design and performance of an Anderson-technique based alignment system”, submitted to *Journal of Physics: Conference Series (Amaldi 6)*.
- [6] D. Z. Anderson, “Alignment of resonant optical cavities”, *Appl. Opt.* **23** (1984) 2944-2949 .
- [7] F. Acernese *et al.* [Virgo Collaboration], “A local control system for the test masses of the Virgo gravitational wave detector”, *Astrop. Phys.* **20** (2004) 617-628 .
- [8] F. Acernese *et al.* [Virgo Collaboration], “The Automatic Alignment System in Virgo”, submitted to *Journal of Physics: Conference Series (Amaldi 6)*.
- [9] F. Acernese *et al.* [Virgo Collaboration], “Automatic mirror alignment for Virgo: First experimental demonstration of the Anderson technique on a large-scale interferometer”, arXiv:gr-qc/0411116.